Theory and Design of an Edge-Coupled Terahertz Photomixer Source

Daryoosh Saeedkia and Safieddin Safavi-Naeini

***Abstract*— A terahertz photomixer with guided-wave optical excitation scheme is analyzed, and as an example, an edge-coupled photomixer source is designed with low-temperature-grown (LTG) GaAs as its ultra-fast photoabsorbing layer and $Al_{0.2}Ga_{0.8}As$ and $Al_{0.35}Ga_{0.65}As$ as core and cladding layers of its optical waveguide structure, respectively.**

***Index Terms*— Terahertz optoelectronics, Photomixers, CW terahertz sources, Optical waveguides.**

I. Introduction

TERAHERTZ technology is a fast-growing field [1], [2] with applications in biology and medicine [3]-[5], medical imaging [6], material spectroscopy and sensing [7], security [8], monitoring and spectroscopy in pharmaceutical industry [9], and high-data-rate communications [10]. The direction of the terahertz technology is towards the implementation of compact and cost-efficient systems for different terahertz applications. Realization of a compact, high-power, and low-cost terahertz source is a crucial step towards this goal.

Photomixers are promising continuous-wave terahertz sources as potentially compact, low-power-consuming, coherent, low-cost, and tunable sources [11], [12]. In a terahertz photomixer, a beat-frequency signal is generated due to mixing of two frequency-detuned laser beams inside a dc-biased ultra-fast photoconductor [13], [14] or a superconductor [15], [16].

Terahertz photomixers can be realized as vertically illuminated or edge-coupled devices [17]-[22]. In the edge-coupled photomixer sources, the laser beams are guided inside an optical dielectric waveguide structure and being absorbed by an overlying ultra-fast photoabsorbing layer, wherein a terahertz signal is generated due to photomixing phenomena. The generated terahertz signal is guided by a transmission line, which can be a coplanar stripline (CPS), a coplanar waveguide (CPW), or a parallel-plate waveguide. The edge-coupled photomixer sources are attractive for system-on-chip configurations for terahertz spectroscopy and sensing and terahertz imaging applications.

Among the challenging issues for realization of the edge-coupled photomixer sources are: control over the optical power absorption rate inside the photoabsorbing layer in order to increase the thermal failure threshold of the device and maximize the generated terahertz power; realization of the velocity match between the optical beat signal and the terahertz signal; and implementation of a proper dc-bias configuration and terahertz waveguiding structure.

This work was supported by the NSERC/RIM Industrial Research Chair Program, and CITO.

The authors are with the Electrical and Computer Engineering Department, University of Waterloo, Waterloo, ON, Canada (email: daryoosh@maxwell.uwaterloo.ca; safavi@maxwell.uwaterloo.ca).

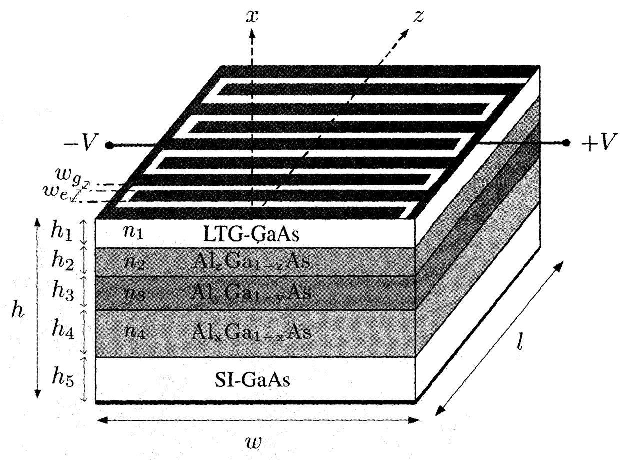

Fig. 1. Schematic of a terahertz photoconductive photomixer source with guided-wave optical excitation. For this structure $n_1 > n_3 > n_2 = n_4$.

In this paper, we analyze an edge-coupled terahertz photomixer source, which contains an optical waveguide structure located above a grounded dielectric substrate and covered by interdigitated electrodes (Fig. 1). The top layer of the optical waveguide structure is made of an ultra-fast photoabsorbing material, wherein the photomixing phenomena takes place. One can control the optical power absorption rate by changing the thickness of the photoabsorbing layer. The dc bias is applied through the interdigitated electrodes. The electrode spacing is much smaller than the wavelength of the generated terahertz signal, hence, it is a good approximation to assume that the terahertz wave sees the electrode structure as a uniform metallic plate. The electrodes and the ground plane act as a parallel-plate waveguide for the generated terahertz signal. The velocity of the terahertz signal along the parallel-plate waveguide and the velocity of the optical signal are close together ($n_{GaAs} = 3.68$ and 3.61 at $\lambda = 800$ nm and $\lambda = 300$ μm, respectively [2]), which results in a good coupling between the two signals.

II. Optical Waveguide

In the configuration shown in Fig. 1, two laser beams with their central frequency difference falling in the terahertz spectrum are coupled to a five-layer dielectric slab waveguide structure. The band gap for $Al_\xi Ga_{1-\xi}As$ is E_g =1.42 eV, 1.66 eV, and 1.86 eV, for $\xi = 0$, $\xi = 0.2$, and $\xi = 0.35$, respectively

[23]. Hence, for the central wavelengths of the two lasers around 780 nm (E = 1.59 eV) the optical power absorption only takes place inside the LTG-GaAs layer. The thickness of the $Al_xGa_{1-x}As$ buffer layer, h_4, is large enough to prevent the evanescent tail of the propagating mode reaching to the SI-GaAs substrate.

Satisfying the following conditions together guarantees the single-mode operation of the five-layer dielectric waveguide

$$h_1 \leq \frac{\lambda \tan^{-1}\left(\sqrt{\frac{n_2^2-n_0^2}{n_1^2-n_2^2}}\right)}{2\pi\sqrt{n_1^2-n_2^2}} \quad (1)$$

$$h_3 \leq \frac{\lambda}{2\sqrt{n_3^2-n_2^2}} \quad (2)$$

$$h_2 > \lambda \quad (3)$$

For $h_2 < \lambda$, it is also possible to design the optical waveguide as a single mode waveguide, however, in this case the behavior of the dispersion equation becomes complicated and it is difficult to extract general conditions for the single mode operation of the waveguide. In a single mode structure, it is easier to achieve both weak coupling to the photoabsorbing layer and velocity phase match between the terahertz signal and the propagating optical mode.

For the structure shown in Fig. 1, we choose the Al contents of the $Al_\xi Ga_{1-\xi}As$ layers as $x = z = 0.35$ and $y = 0.2$. At the wavelength $\lambda = 780\ nm$ (E = 1.59 eV) the refractive index of the layers in Fig. 1 will be $n_1 = 3.66$, $n_2 = n_4 = 3.44$, and $n_3 = 3.554$.

The bias electrodes are made of gold with the refractive index $n_0 = 0.1383 - j4.7932$ at $\lambda = 780$ nm.

The total thickness of the dielectric region, h, must be small enough so that only TEM mode can be supported by the parallel-plate waveguide. This can be achieved by

$$h \leq \frac{c}{2f_c n_1} \quad (4)$$

where f_c is the cutoff frequency of the lowest order non-TEM modes. For example, for $h \leq 6.8\ \mu m$ and for the frequencies below 6 THz, the only supported mode by the parallel-plate waveguide is the TEM mode.

The optical intensity distribution across the dielectric layers and at the different positions along the waveguide is shown in Fig. 2. As it can be seen from Fig. 2, the optical intensity decreases as the optical field propagates along the waveguide, which is due to the optical power absorption inside the LTG-GaAs layer.

Fig. 3 shows the total optical power inside the waveguide along the z-axis and optical intensity distribution of TE_0 mode across the dielectric layers for different values of h_1, h_2, and h_3. The total optical power decreases exponentially along the waveguide. The following equation fits the resulting graphs

$$P_{opt}(z) = P_{opt}(z=0)e^{-\alpha_e z} \quad (5)$$

where $\alpha_e < \alpha$ is the effective absorption coefficient. For the higher optical intensity inside the photoabsorbing layer, the effective absorption coefficient is higher. The optical power

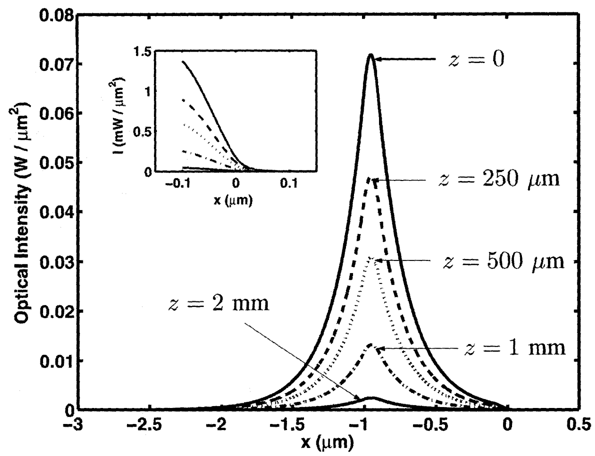

Fig. 2. Optical intensity distribution of TE_0 mode across the dielectric layers and at the different positions along the waveguide. The thicknesses of the dielectric layers in Fig. 1 are $h_1 = 100\ nm$, $h_2 = 800\ nm$, $h_3 = 100\ nm$, and $h_4 = 2\ \mu m$. The width of the waveguide is $w = 6\ \mu m$. The optical power of each laser is 200 mW. The width of the electrode fingers and the gap between them are $w_e = w_g = 2\ \mu$m. The propagation constants in the conductor-covered and air-covered regions are $\beta = 2.7813 \times 10^7$ rad/m and $\beta = 2.7814 \times 10^7$ rad/m, respectively. Inset shows the optical intensity inside the photoabsorbing layer and air.

inside the LTG-GaAs layer decays at the same rate as the total optical power.

III. Simulation Results

All the physical and dimensional parameters of the designed photomixers are given in Table I. For the designed devices, the ultra-fast photoabsorbing layer is LTG-GaAs and Al contents of the $Al_\xi Ga_{1-\xi}As$ layers are $x = z = 0.35$ and $y = 0.2$ (see Fig. 1). The propagation constants of the two laser modes in the air-covered region for the beat frequency of 1 THz are $\beta_1 = 2.7815 \times 10^7$ rad/m and $\beta_2 = 2.7742 \times 10^7$ rad/m.

Fig. 4 shows the terahertz photocurrent along the waveguide at 1 THz beat frequency and at different depths. The total static electric field is shown for comparison. The terahertz photocurrent is lower at the surface of the LTG-GaAs layer, where the optical intensity is smaller (see Fig. 2). The amplitude of the x-component of the terahertz photocurrent are smaller under the electrodes, where the amplitude of the electric field is low. As it can be seen from Fig. 4, the terahertz photocurrent follows the static electric field variation in low-field regime. For the static field above a certain value the carrier velocity saturates and the carrier lifetime become big enough to make $\Omega\tau >> 1$, hence the terahertz photocurrent becomes independent of the electric field.

Fig.4 also shows the x-component of the terahertz photocurrent along the waveguide at two different beat frequencies. For the beat frequency f = 0.1 THz, the terahertz photocurrent follows the static electric field variation even at the high-field regime. This is due to the fact that at the low frequencies the term $\Omega\tau$ is small and the terahertz photocurrent is proportional to the carrier lifetime and hence is a function of the electric field. For the beat frequency f = 1 THz, and except for

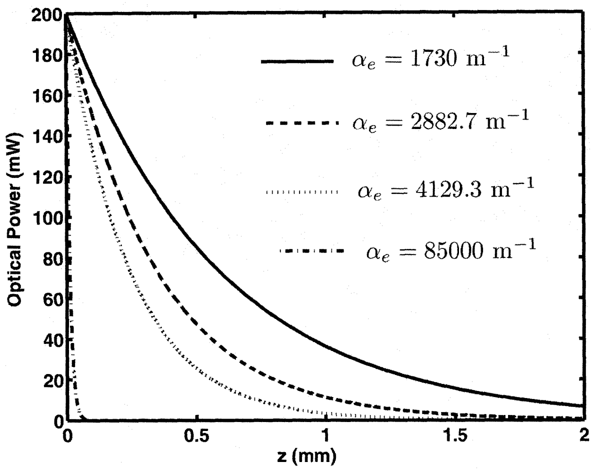

(a)

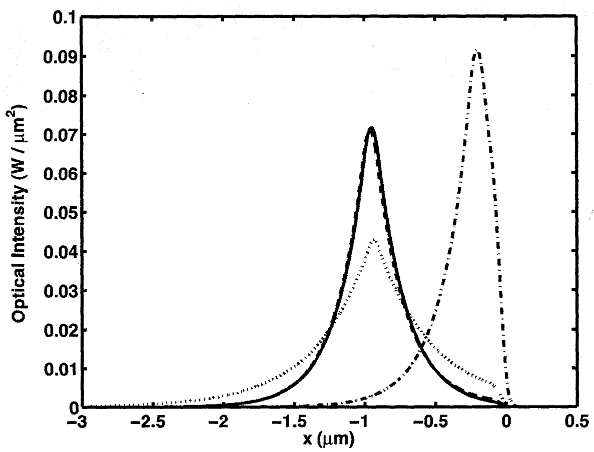

(b)

Fig. 3. Total optical power inside the waveguide along the z-axis and optical intensity distribution of TE_0 mode across the dielectric layers for different values of h_1, h_2, and h_3 and with $h_4 = 2\ \mu$m: $(h_1, h_2, h_3) = (100, 800, 100)$ nm (solid line), $(h_1, h_2, h_3) = (110, 800, 100)$ nm (dashed line), $(h_1, h_2, h_3) = (100, 800, 50)$ nm (dotted line), and $(h_1, h_2, h_3) = (100, 50, 100)$ nm (dash-dot line). The width and the length of the waveguide are $w = 6\ \mu$m and $l = 2$ mm, respectively. The width of the electrode fingers and the gap between them are $w_e = w_g = 2\ \mu$m. The input optical power is 200 mW.

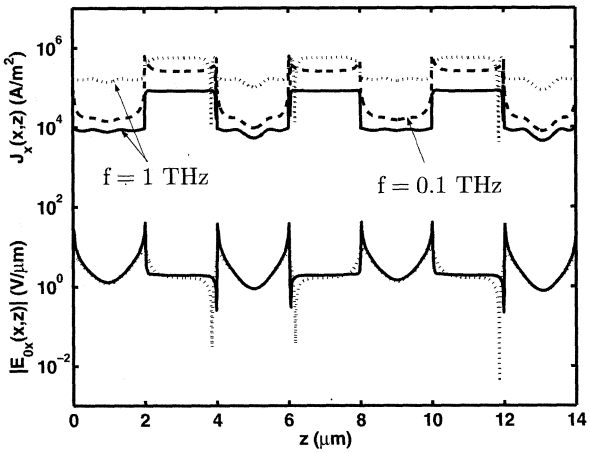

Fig. 4. Terahertz photocurrent along the waveguide at different beat frequency and at different depths: $x = -10$ nm, f = 1 THz (solid line), $x = -10$ nm, f = 0.1 THz (dashed line), and $x = -110$ nm, f = 1 THz (dotted line). The thicknesses of the dielectric layers are: $h_1 = 100$ nm, $h_2 = 800$ nm, $h_3 = 100$ nm, and $h_4 = 2\ \mu$m. The static electric field is shown for comparison.

TABLE I
PHYSICAL AND DIMENSIONAL PARAMETERS OF A DESIGNED PHOTOMIXER

Description	Notation	Value
Laser central wavelength	λ_1	780 nm
Applied dc voltage	V	10 V
Each laser power	P_{opt}	200 mW
Optical absorption coefficient[24]	α	10000 cm^{-1}
Electron (hole) saturation velocity[25]	v_{sn} (v_{sp})	40 (10) m/ms
Low-field electron (hole) lifetime[25]	τ_n (τ_p)	0.1 (0.4) ps
Low-field electron (hole) mobility[26]	μ_{n0} (μ_{p0})	400 (100) cm^2/Vs
Device width	w	6 μm
Total thickness	h	6 μm
Electrode width	w_e	2 μm
Gap between electrode fingers	w_g	2 μm
Buffer layer thickness	h_4	2 μm
LTG-GaAs refractive index	n_1	3.66
Cladding refractive index	n_2, n_4	3.44
Core refractive index	n_3	3.554
Electrode refractive index (at 780 nm)	n_0	$0.1383 - j4.7932$

very low electric field, the term $\Omega\tau$ becomes large and hence the terahertz photocurrent becomes independent of the electric field. One can see from Fig. 4 that the terahertz photocurrent is higher inside the air-covered regions, where the optical intensity is higher.

Fig. 5 shows the amplitude of the x-components of the terahertz photocurrent and the dc photocurrent for different values of the thicknesses of the dielectric layers. As it can be seen from Fig. 5, both the terahertz photocurrent and the dc photocurrent are higher when the coupled optical power inside the photoabsorbing layer is higher (see Fig. 3). Since the generated terahertz power is proportional to the square of the terahertz photocurrent, one can increase the generated terahertz power by increasing the coupled optical power inside the photoabsorbing layer. Hence, the optimum thicknesses for the dielectric layers are the thicknesses, which results in maximum possible optical intensity inside the LTG-GaAs layer. Nevertheless, one has to take into account the device thermal failure due to the resulting optical and electrical thermal power.

The generated terahertz power for an edge-coupled photomixer with parameters given in Table I and with $h_1 = h_3 = 100$ nm and $h_2 = 50$ nm is 0.9 μW at 1 THz beat frequency.

IV. Conclusion

An edge-coupled distributed terahertz photomixer source is analyzed and designed. The proposed device has potential applications in terahertz biosensing, imaging, and spectroscopy.

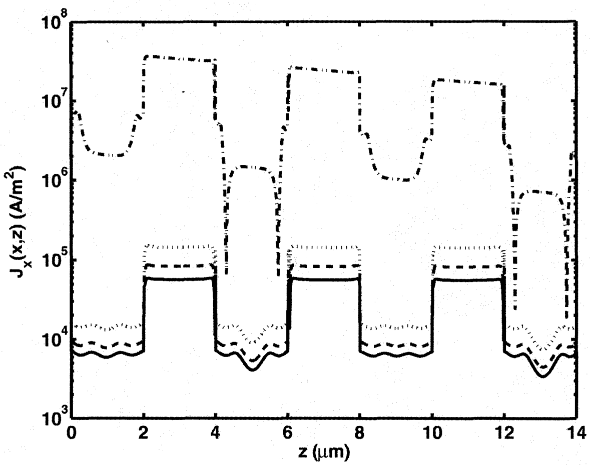

(a)

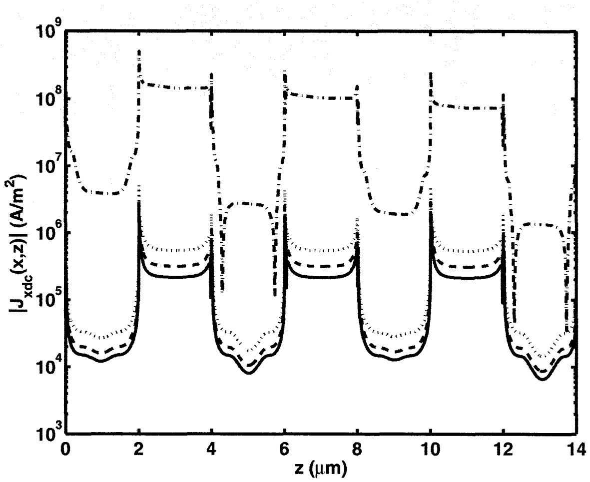

(b)

Fig. 5. Generated photocurrent along the waveguide at 1 THz beat frequency and at $x = -10$ nm for different values of h_1, h_2, and h_3 and with $h_4 = 2$ μm: $(h_1, h_2, h_3) = (100, 800, 100)$ nm (solid line), $(h_1, h_2, h_3) = (110, 800, 100)$ nm (dashed line), $(h_1, h_2, h_3) = (100, 800, 50)$ nm (dotted line), and $(h_1, h_2, h_3) = (100, 50, 100)$ nm (dash-dot line). (a) terahertz photocurrent (b) dc photocurrent.

REFERENCES

[1] D. L. Woolard, E. R. Brown, M. Pepper, and M. Kemp, "Terahertz Frequency Sensing and Imaging: A Time of Reckoning Future Applications?" *Proceedings of the IEEE*, vol. 93, no. 10, pp. 1722–1743, 2005.

[2] K. Sakai, Ed., *Terahertz Optoelectronics*. Springer-Verlag, 2005.

[3] M. Nagel, P. Haring Bolivar, and H. Kurz, "Modular parallel-plate THz components for cost-efficient biosensing systems," *Semicond. Sci. Technol.*, vol. 20, no. 7, pp. S281–S285, 2005.

[4] P. H. Siegel, "Terahertz Technology in Biology and Medicine," *IEEE Trans. Microwave Theory Tech.*, vol. 52, no. 10, pp. 2438–2447, 2004.

[5] T. Globus, D. Woolard, M. Bykhovskaia, B. Gelmont, L. Werbos, and A. Samuels, "THz-frequency spectroscopic sensing of DNA and related biological materials," *International Journal of High Speed Electronics and Systems*, vol. 13, no. 4, pp. 903–936, 2003.

[6] S. Wang, B. Ferguson, D. Abbott, and X.-C. Zhang, "T-ray imaging and tomography," *J. Biol. Phys.*, vol. 29, no. 2-3, pp. 247–256, 2003.

[7] D. Mittleman, Ed., *Sensing with Terahertz Radiation*. Springer-Verlag, 2003.

[8] M. C. Kemp, P. F. Taday, B. E. Cole, J. A. Cluff, A. J. Fitzgerald, and W. R. Tribe, "Security applications of terahertz technology," in *The Proceedings of SPIE Conference*, vol. 5070, August 2003, pp. 44–52.

[9] P. F. Taday, "Applications of terahertz spectroscopy to pharmaceutical sciences," *Phil. Trans. R. Soc. Lond. A*, vol. 362, no. 1815, pp. 351–364, 2004.

[10] A. Hirata, H. Ishii, and T. Nagatsuma, "Design and characterization of a 120-GHz millimeter-wave antenna for integrated photonic transmitters," *The Proceedings of International Topical Meeting on Microwave/Photonics*, pp. 229–232, 2000.

[11] M. C. Teich, "Field-Theoretical Treatment of Photomixing," *Appl. Phys. Lett.*, vol. 14, no. 6, pp. 201–203, 1969.

[12] E. R. Brown, F. W. Smith, and K. A. McIntosh, "Coherent millimeter-wave generation by heterodyne conversion in low-temperature-grown GaAs photoconductors," *J. Appl. Phys.*, vol. 73, no. 3, pp. 1480–1484, 1993.

[13] E. R. Brown, "THz Generation by Photomixing in Ultrafast Photoconductors," *International Journal of High Speed Electronics and Systems*, vol. 13, no. 2, pp. 497–545, 2003.

[14] D. Saeedkia, R. R. Mansour, and S. Safavi-Naeini, "The interaction of laser and photoconductor in a continuous-wave terahertz photomixer," *IEEE J. Quantum Elec.*, vol. 41, no. 9, pp. 1188–1196, 2005.

[15] C. J. Stevens and D. J. Edwards, "Photomixing receiver using kinetic inductive effect in high T_c superconductors," *Electronics Letters*, vol. 37, no. 23, pp. 1420–1421, 2001.

[16] D. Saeedkia, R. R. Mansour, and S. Safavi-Naeini, "Modeling and Analysis of High-Temperature Superconductor Terahertz Photomixers," *IEEE Trans. Appl. Superconduct.*, vol. 15, no. 3, pp. 3847–3855, 2005.

[17] E. A. Michael, "Travelling-wave photonic mixers for increased continuous-wave power beyond 1 THz," *Semicond. Sci. Technol.*, vol. 20, no. 7, pp. S164–S177, 2005.

[18] H. Ito, S. Kodama, Y. Muramoto, T. Furuta, T. Nagatsuma, and T. Ishibashi, "High-Speed and High-Output InP-InGaAs Unitraveling-Carrier Photodiodes," *IEEE J. Sel. Top. Quantum Electron.*, vol. 10, no. 4, pp. 709–727, 2004.

[19] E. Peytavit, S. Arscott, D. Lippens, G. Mouret, S. Matton, P. Masselin, R. Bocquet, J. F. Lampin, L. Desplanque, and F. Mollot, "Terahertz frequency difference from vertically integrated low-temperature-grown GaAs photodetector," *Appl. Phys. Lett.*, vol. 81, no. 7, pp. 1174–1176, 2002.

[20] J.-W. Shi, K.-G. Gan, Y.-J. Chiu,Y.-H. Chen, C.-K. Sun, Y.-J. Yang, and J. E. Bowers, "Metal-semiconductor-metal traveling-wave photodetectors," *IEEE Photon. Technol. Lett.*, vol. 16, no. 6, pp. 623–625, 2001.

[21] L. Y. Lin, M. C. Wu, T. Itoh, T. A. Vang, R. E. Muller, D. L. Sivco, and A. Y. Cho, "High-Power High-Speed Photodetectors-Design, Analysis, and Experimental Demonstration," *IEEE Trans. Microwave Theory Tech.*, vol. 45, no. 8, pp. 1320–1331, 1997.

[22] E. H. Bottcher and D. Bimberg, "Millimeter wave distributed metal-semiconductor-metal photodetectors," *Appl. Phys. Lett.*, vol. 66, no. 26, pp. 3648–3650, 1995.

[23] T. Tamir, Ed., *Guided-Wave Optoelectronics*. Springer-Verlag, 1988.

[24] S. M. Sze, *Physics of Semiconductor Devices*. John Wiley and Sons, 1981.

[25] E. R. Brown, "A photoconductive model for superior GaAs THz photomixer," *Appl. Phys. Lett.*, vol. 75, no. 6, pp. 769–771, 1999.

[26] E. R. Brown, K. A. McIntosh, F. W. Smith, K. B. Nichols, M. J. Manfra, C. L. Dennis, and J. P. Mailia, "Milliwatt output levels and superquadratic bias dependence in a low-temperature-grown GaAs photomixer," *Appl. Phys. Lett.*, vol. 64, no. 24, pp. 3311–3313, 1994.